Tribology in Industry

Mechanical Properties and Analysis of Two-body Abrasive Wear Behaviour of Graphene Modified Carbon/Epoxy Composites Using Taguchi's Technique

Anupama Shivamurthy[a], Rakshith Boranna[b], Raviprasad Kogravalli Jagannat[c], Gurusiddappa R. Prashanth[d], Suresha Bheemappa[e,*], S.M. Darshan[f]

[a]*Department of Electronics and Communication Engineering, National Institute of Technology, Goa, Goa-403401, India,*
[b]*Department of Electronics and Communication Engineering, JSS Science and Technology University, Mysuru-570006, Karnataka, India,*
[c]*Department of Applied Science, National Institute of Technology Goa, Goa-403401, India,*
[d]*Department of Electronics and Communication Engineering, National Institute of Technology, Goa, Goa-403401, India,*
[e]*Department of Mechanical Engineering, The National Institute of Engineering, Mysuru-570008, Karnataka, India,*
[f]*Department of Mechanical and Automobile Engineering, CHRIST (Deemed to be University), Bengaluru-570008, Karnataka, India.*

A B S T R A C T

The present work emphasizes the effect of graphene nanoplatelets (G) filler loading on mechanical and abrasive wear behavior of carbon fibre reinforced epoxy (C/E) composites. Graphene nanoplatelets were mixed with epoxy framework using a temperature-controlled magnetic stirrer and then ultrasonically treated. The parameters considered for the abrasive wear study are the applied load in N (5, 10 and 15), abrading distance in m (75, 150, and 225) and weight percentage of reinforcement (0, 1, and 1.5). The incorporation of 1 wt. % G into C/E composites increases hardness by 14 % and interlaminar laminar strength by 19 % when compared to C/E composites. According to the Taguchi design of tests, a filler loading of 1 wt. % G, an abrading distance of 225 m, and an applied load of 15 N are ideal. Analysis of variance (ANOVA) was done to establish the dominant parameter, and the filler loading with abrading distance was shown to be significant. With 36.4 %, the filler loading had the biggest influence on the composite specific wear rate. The combination of filler loading with 1 wt. %, load of 15 N, and abrading distance of 225 m yields the lowest specific wear rate. The involved wear mechanisms during the abrasive wear process have also been explained with scanning electron micrographs.

1. INTRODUCTION

Normally, metals and polymers have been competing in the manufacturing of vehicles. Polymer-based composite materials are taking the place of traditional materials (metals, alloys, and ceramics) due to their ease of processing and productivity [1]. In contrast, multiphase polymer-based composite materials provide exceptional strength-to-weight ratio, damage tolerance, fatigue, corrosion resistance, and wear resistance, making them excellent alternatives for conventional materials used in bearing or moving components. Polymer-based composite materials filled with nanofillers offer greater strength and stiffness, which are often the most important characteristics for numerous applications, including complex structures in aerospace, automotive, electrical, marine, biomedical, and chemical components [2]. Man-made fibres such as carbon, glass, basalt, and Kevlar are extensively utilized in the production of polymer-based composite materials. They provide exceptional properties suitable for the aforementioned applications. These fibres possess superior strength and stiffness in comparison to the polymer matrix material, making them highly practical for load-bearing applications in composite structures [3].

Carbon fibre, when used in unidirectional (UD)/bidirectional (B/D) mat form as primary reinforcement, exhibits excellent mechanical, tribological, and thermal properties that are well-suited for aerospace and automotive applications [4]. Polymer-based composite materials are manufactured using polymer matrix materials like polyester, epoxy, vinyl ester, and bismaleimide, which are ideal for producing ballistic armor, bulletproof vests, helmets, and bearing parts [5]. The use of epoxy resin as a matrix material is known to significantly enhance the strength (tensile, flexural, and impact) of mono/hybrid composites (e.g., SiC filled carbon/epoxy and Al_2O_3 filled carbon/epoxy, SiC filled glass/epoxy) parts [6,7]. In PMCs, Although there is a wide range of matrix/binding materials used (Table 1), epoxy resins offer excellent strength which makes them more practical in aerospace, automotive and marine applications [8].

The rubbing of a softer surface by a hard rough surface causes two-body abrasive wear. The wear of polymer and their composites is a complicated occurrence that relies on many factors such as materials, shapes, firmness, durability, crystalline structure, temperature of transformation, arrangement of fibres/fillers, adhesion at the interface, and conditions of tribo-testing [9]. Polymer-based composite materials show considerable improvements in dry conditions. Nevertheless, there is a scarcity of research regarding the abrasive characteristics of polymer-based micro and nanocomposites. Pejakovic and colleagues [10] carried out experiments to assess the resistance of various commercially available polymer materials to abrasion using SiO_2 abrasives. The samples made of polyethylene exhibited greater wear loss, whereas those made of polyurethane showed that abrasion resistance was influenced by both hardness and elongation. Shipway and Ngao [11] investigated the abrasive wear characteristics of several polymeric materials and found that the wear properties were influenced by the type of polymer. Based on these findings, it can be concluded that the wear behavior is determined by the type of polymer.

Several useful fillers at micro and nano scales that can lead to low-cost composites with high wear resistance, mechanical properties and performance are being investigated. The use of solid lubricants can also help in the development of better polymer composite bearings [12]. Carbon/epoxy with functional fillers provide significant properties (physical, mechanical, and tribological) in composite parts and is therefore suitable for a wide range of applications. Graphene is a well-known nanomaterial that has garnered the attention of researchers due to its exceptional qualities. This includes high aspect ratio, remarkable thermal conductivity, impressive mechanical strength, low shear strength, unparalleled friction, and wear properties [13]. Table 1 summarizes the main research efforts connected to the mechanical characteristics and abrasive wear-mode behavior of graphene nanoplatelets (GNPs) modified carbon/glass fabric-thermoset matrix composites. As listed in Table 1, Wang et al. [14] investigated the influence of GNPs with two different lateral dimensions on the morphological, flexural, and thermo-mechanical characteristics of multiscale GNPs with glass fibre reinforced epoxy (GNPs/G/E) composites (GnP-C750; 1 μm in diameter and GnP-

5.5 µm in diameter). Calendaring and sonication methods are used in the manufacturing process. They found that the flexural modulus of the GNPs/G/E composites was enhanced by 11.5 and 26.3 %, respectively, with the addition of 5 wt. % GnP-C750 and GnP-5.

Kumar et al. [15] examined the effect of various wt. % of GNPs on the mechanical and abrasive wear behavior of G/E composites. According to the findings of the current study, the introduction of GNPs can increase the performance of G/E composites. Furthermore, they found that the inclusion of a considerable amount (1 wt. %) of GNPs significantly improved the tribo-performance, interlaminar shear strength, and hardness of the composites. In another work by the same authors group [16] found that inclusion of 1 wt. % GNPs into G/E resulted in the lowest wear rate (2.31×10^{-11} m³/N m). Furthermore, the inclusion of 0.5 and 1.0 wt. % GNPs in G/E reduced CoF by around 4% and 18%, respectively. for abrading distance of 200 m, due to the self-lubricity of GNPs.

Srivastava et al. [17] desized and oxidised carbon fibres, as well as coated them with GNPs, with the goal of strengthening the interface/interphase between the fibre and the matrix. The experimental results show that the flexural strength of the laminates improved dramatically with GNPs addition. Shivakumar et al. [18] investigated the mechanical characteristics (tensile, flexural, and impact strengths) of GNPs in C/E composites.

Namdev et al. [19] studied the influence of varied GNPs weight percentages on mechanical and physical properties. They found that 0.5 wt. % GNPs had greater tensile, flexural, shear, and impact strength, hardness, than unfilled and 0.3 and 0.7 wt. % GNPs/C/E composites. Mechanical characteristics were observed to be reduced over 0.7 wt. % of GNPs due to nanoparticle aggregation in the composites. GNPs were observed to increase the tribo-performance of neat epoxy and C/E composites in various studies [20-23].

Table 1. Recent research works related to mechanical properties and abrasive wear-mode behavior of graphene modified glass/carbon fabric-epoxy composites.

Composite constituents	Processing method	Research highlights	Ref.
GNPs/G/E	Hand lay-up method	Inclusion of 5 wt. % GNPs increased the flexural modulus and strength by 26.3 % and 16.2% respectively.	[14]
GNPs/G/E	Hand lay-up and compression moulding	1 wt. % of GNPs enhanced the tribo-performance, interlaminar shear strength and hardness of composites	[15]
GNPs/G/E	Hand lay-up and compression moulding	Addition of 1 wt. % GNPs reduced the wear rate from 4.54×10^{-11} m³/Nm (G/E) to the lowest value of 2.31×10^{-11} m³/Nm. CoF of 0.5 and 1.0 wt. % of GNPs lowered by 4% and 18% respectively.	[16]
GNPs/C/E	Vacuum assisted resin transfer moulding	GNPs inclusion improved the flexural strength.	[17]
GNPs/C/E	Compression moulding	The maximum values were obtained with the inclusion of 0.5 wt. % of GNPs. The tensile and flexural strengths were enhanced by 11% and 18% respectively.	[18]
GNPs/C/E	Hand layup and vacuum bagging	Inclusion of GNPs improved the mechanical properties.	[19]
GNPs/C/E	Hand lay-up/compression moulding	Addition of 0.5 wt. % GNPs augmented the tensile and flexural strengths as well as reduced the wear loss.	[20]
carboxylic acid (COOH) functionalized graphene (CGr)/epoxy	Open moulding	Epoxy with 0.6 wt. % of CGr reduced the CoF and increased the wear resistance.	[21]
GNPs/C/E	Hand layup and compression moulding	Incorporating 0.5 wt. % GNPs significantly improved the wear performance.	[22]
GNP/C/E	Hand layup, compression molding	Inclusion of GNPs had reduced the weight loss, CoF, and wear rate. These tribological properties decreased as the wt. % of GNPs increased.	[23]

Several studies have been conducted to examine the mechanical properties of GNPs modified C/E hybrid composite systems. However, as far as we know, the synergistic effect of GNPs and UD carbon fibre on the two-body abrasive wear properties of epoxy-based hybrid nanocomposites has not been studied. The present manuscript focuses on the abrasive wear of C/E composites filled with GNPs, specifically two-body wear-mode. The article is structured as follows: Section 2 provides an overview of composite fabrication and pin-on-disc wear experiments. This is followed by a discussion of the experimental findings. Section 3 delves into the specific wear rate of effect of GNPs loading into C/E composites, with an analysis of the results and discussion. Lastly, Section 4 presents the concluding remarks.

2. MATERIALS AND METHODS

2.1 Materials

The constituents of the multiphase composites are i) the main phase is epoxy matrix (Epon 828, denoted as E), ii) the primary strengthening phase is carbon fabric (3 K, UD, denoted as C), and iii) the secondary strengthening phase is graphene nanoplatelets (xGnP-25, denoted as G). EPON™ resin 828 is an undiluted clear difunctional bisphenol A/epichlorohydrin derived liquid epoxy resin. Because of its wide range of uses in polymer composite constructions for automotive and aerospace applications, Epon 828 epoxy matrix was chosen as the major continuous phase. Epicure W, an aromatic amine curing agent with an amine hydrogen equivalent weight (AHEW) of 43 - 46 gmol^{-1}, was chosen as the curing agent.

Epon 828 has a dynamic viscosity of 100 - 300 cP and functions as a curing agent at higher temperatures. According to the supplier, the mixing ratio of Epon 828 to Epicure W was 100:26.4 by weight. Miller-Stephenson Inc. provided these items. XG Sciences Inc. provided the graphene nanoplatelets (xGnP M-25). Graphene nanoplatelets have a thickness of 6 - 10 nm, a surface area of 120 - 150 m^2 g^{-1}, and an average particle diameter of 25 nm. Table 2 shows the characteristics of the elements employed in the manufacture of hybrid nanocomposites.

Table 2. Properties of the constituents of the composites.

Material	Property	Magnitude
Epon 828	Dynamic viscosity (Pa.s)	12–14
	Density (g/cm³)	1.16
	Flashpoint (ᵒC)	200
	Boiling point (ᵒC)	200
G	Diameter (nm)	25
	Purity (%)	95
Carbon fibre	Density (g/cm³)	1.79
	Areal density(g/m²)	372
	Tensile strength (MPa)	2100-3900
	Young's modulus (GPa)	200-245
	Shape and size (μm)	Cylindrical and 7

2.2 Fabrication of composites

The schematic of the 24-ply laminate fabricated is shown in Fig. 1. The required layers of prepreg for fabrication were based on the thickness of the laminate. A quasi-isotropic laminate of stacking sequence $(-45/90/45/0)_{3S}$ was used for fabricating the 24-ply carbon fibre- epoxy (C/E) and GNPs-carbon fibre-epoxy (G/C/E) laminates based on fabrication method followed by Shivakumar et al. [24].
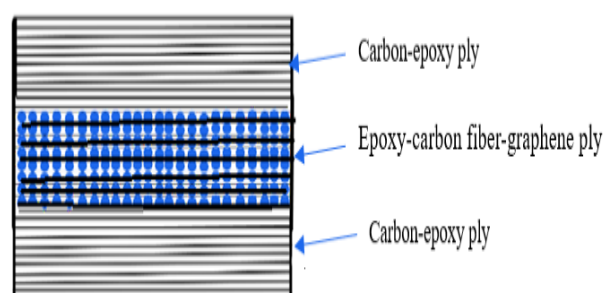

Fig. 1. Schematic of the stacking arrangement of 24-ply laminate.

Complete stacking sequence of the laminate is shown in Fig. 2(a). The central 8-ply GNPs-carbon fibre-Epoxy prepreg is sandwiched between two 8-ply carbon fibre-epoxy prepreg on either side. The stacked prepreg layers are placed between two PTFE films, and by bagging, a vacuum of 100 kPa is applied. The debulked prepreg is then used for moulding. The laminates were fabricated in an autoclave (using a pressure of 700 kPa and temperature of 177 ᵒC). The temperature and pressure cycle used for fabrication is depicted in Fig. 2(b). The thickness variations of ten measurements were within 4.15± 0.02 mm. Laminates were examined for external damage and were also subjected to c-scan to ensure there is no internal damage.
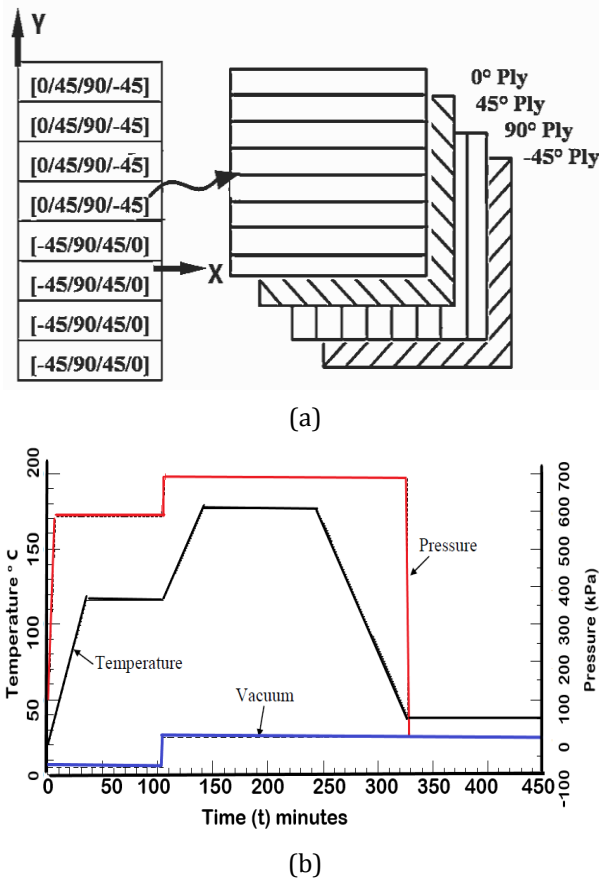
(a)

(b)

Fig. 2. (a) Stacking sequence, (b) Temperature-Pressure-Vacuum cycle used for fabrication.

The different stages of the fabrication of the laminates consisted of (i) cutting of the prepreg and butting, (ii) stacking and debulking, and (iii) mould preparation and bagging.

2.3 Hardness test

Shore hardness meter (Shore-D) is one of the most often used instruments for measuring the hardness of polymeric-based composite materials. The hardness was determined by measuring the depth of a notch created by an inflexible ball under a spring force, and then converting the notch to hardness degrees on a circular scale ranging from 0 to 100. The hardness scale of 0 to 100 is chosen so that "0" represents a rubber with a zero flexible modulus and "100" represents an elastic with an infinitely variable modulus. Hardness testing were carried out in accordance with the ASTM D2240 standard. Hardness measurements were taken at 10 distinct sites, and the mean hardness value for each coupon was computed.

2.4 Short beam shear test

The short beam shear test is used to examine the matrix adhesion quality. This is similar to the three-point bend test. However, the coupon length of the short beam is shorter than that of the flexural coupon. As a result, the vertical force causes shear stress in the plane of the specimens. The ASTM D2344 standard requires the coupon to have accurate geometrical and dimensional tolerances. To meet these requirements, a high precision cutting machine (Mitre Saw, 2200W) equipped with a diamond saw was employed. The interlaminar shear strength (ILSS) tests were carried out using a universal testing machine (Instron UTM; 6800 Series) with a 10 kN load cell. All the tests were carried out at room temperature. The crosshead speed was adjusted to one millimetre per minute, and the interlaminar shear strength was determined using the equation (1):

$$ILSS = 0.75 \times \frac{F_{max}}{A} \qquad (1)$$

where ILSS is the interlaminar shear strength in N mm^{-2}, F_{max} is the maximum force in N, and A is the surface area of the coupon in square mm.

2.5 Experimental design

The optimum composite composition was established as well as the number of runs for testing was decreased using Taguchi's DOE. This method is frequently employed for quality attribute optimization with different combinations of the input variables. It thus produces the minimum variation by reduce the number of experiments as compared to Response Surface Methodology (RSM). To conduct experimental runs employing such a potent analysis tool, Minitab 19 software is employed. Table 3 lists a number of controls that could influence Taguchi's system's response effectiveness.

The three variables and three levels have been chosen for the L$_9$ orthogonal array. Taguchi orthogonal array (L$_9$) is one of the most efficient methods for multifactor optimizing conditions. It is used to achieve the best response under the studied tribological conditions. In addition, it designs the experiment process that allow for the independent evaluation of factors through a small number of trials. Signal to Noise evaluation (S/N)

has produced three different types of quality loss functions: nominally better, higher is better, and lower is better. The most optimum/effective wear-rate characteristics were thus obtained using the lower is better function.

Table 3. Process parameters and their levels.

Sl. No.	Factors	Level		
		1	2	3
1	Filler loading (wt. %)	0	1.0	1.5
2	Applied load (N)	5	10	15
3	Abrading distance (m)	75	150	225

2.6 Two-body abrasive wear test

To determine the wear behaviour of the G/C/E composites, a Pin-on-Disk with a SiC-emery paper embedded to the counter face was used. A graphic representation of the two-body abrasive wear test is depicted in Fig. 3. In this investigation, silicon carbide (SiC) emery papers (320 grit ≈ 32-36 μm) fixed on a rotating steel disc were used as the modified counter face. The specimens were loaded against the modified counter face. Three series of composites viz., C/E, 1G/C/E and 1.5G/C/E were tested in the investigation.
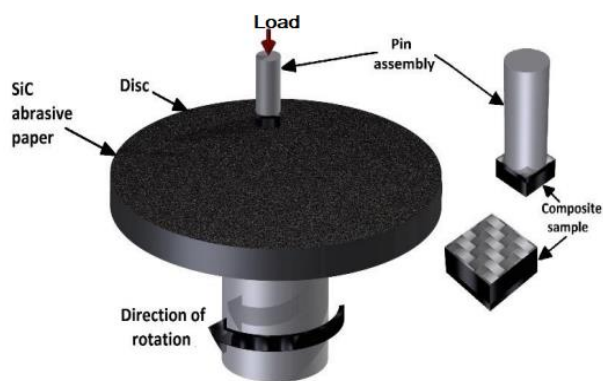

Fig 3. Graphic representation of the two-body abrasive wear test

Two-body abrasive wear tests were conducted at room temperature as per ASTM G-99. The test coupons were abraded under the tribo-parameters listed in Table 2. The test coupons are of size of 6 mm × 6 mm × 3 mm glued to the aluminium cylindrical pin of 6 mm diameter and 25 mm length were prepared. The constant sliding velocity of 0.5 m/s, track diameter of 100 mm and emery paper of 320 grit was used for all tests. Before each test, the wear surface of a coupon was ground with the 600-grit abrasive paper, making

sure that each of the coupons had the same contact area and surface roughness. A new abrasive paper was used for each of the tests. Before and after every test, the specimens were cleaned with acetone and then dried with a heat blower. An electronic balance with a sensitivity of 0.1 mg was used for measuring the masses of the pin coupons. Each test was performed three times and the average of the tests was used. The wear mass loss was obtained from the mass differences for the pin coupon measured before and after the tests. The wear volume loss and specific wear rate (SWR) of the coupons were calculated using the measured densities of the composites.

3. RESULTS AND DISCUSSION

3.1 Hardness

The impact of G loading on the hardness of controlled C/E composites is shown in Table 4. The Shore D hardness of controlled C/E increased to 81 at 1 wt. % G and decreased to 77 (Shore D) at 1.5 wt. % G. The high modulus and aspect ratio of G has resulted in the upward trend. The lowest value of hardness is observed at 1.5 wt. % G. The non uniform dispersion during manufacturing increased as G loading increased. Likewise, hardness tests revealed that the hardness of G/C/E samples is higher than that of controlled C/E composite samples.

Table 4. Density, hardness and interlaminar shear strength of G/ C/E composites.

Composites	Density (g cm⁻³)	Hardness (Shore D)	ILSS (MPa)
C/E	1.48±0.05	71±1	36.3 ±2.1
1G/C/E	1.46±0.03	81±1	43.2±1.9
1.5G/C/E	1.43±0.03	77±1	38.1±2.4

3.2 Interlaminar shear strength

The interlaminar shear strength (ILSS) of nanocomposites reveals the degree of adhesiveness between the fibre and matrix. In general, nanofillers are used to increase the surface area of the interface between the fibre and the matrix, hence increasing the interface strength. The ILSS of controlled C/E and G/C/E composites samples is summarized in Table 4. When comparing G/C/E composites to control C/E composites, it is seen that ILSS has improved. The addition of 1 wt. % G has increased ILSS by 19% in relative to the control C/E composites.

The improvement in ILSS is attributed to an increase in interface strength rather than a decrease in void content. According to the void content study (Table 4), there is a rise in void content % with increasing G loading. The decrease in ILSS with increasing G loading (1.5 wt. %) is attributable to G aggregation, which reduces the effective contact surface area and hence decreases ILSS.

The increased interfacial characteristics of the C/E composites were responsible for the property enhancement. To achieve superior interfacial qualities, a composite slab with a modified epoxy matrix and 1 wt. % G's was reported to boost hardness and ILSS by 14% and 19.3%, respectively, when compared to the controlled C/E composite. The epoxy matrix was combined with G in a temperature-controlled attractive stirrer before being ultrasonically treated, resulting in increased hardness and ILSS. As a result, the use of G enhanced the interaction energy between carbon fibres and the epoxy matrix. Furthermore, functional groups on the surface of carbon fibres, such as hydroxyl and carboxyl groups, reacted with epoxy groups on graphene layers, assisting in the formation of a chemical bond between carbon fibres and graphene layers. Thus, a combination of these factors enhanced the interfacial adhesion between the fibre/matrix interphase [25].

3.3 Statistical analysis of wear results

The abrasive behaviour of G/C/E composites under the two-body mode is examined based on load, filler loading, as well as abrading-distance. The experimental design of Taguchi's L_9 array is

simulated. Fig. 4 and Table 5 display the experimental design as well as findings of two-body abrasion wear of C/E composite filled with G. The pertinent tests for this table are run at a constant speed as well as grit size. The G/C/E composites under research had an average S/N ratio of -22.28 dB. When controlling variables are set with the highest S/N ratio, their optimum output having smallest variance is consistently produced. Fig. 4 shows the trend of the S/N ratio as the control parameter setting was changed from its one level towards the next.
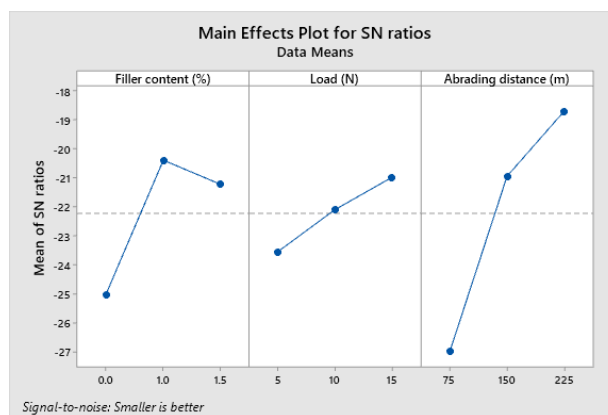

Fig. 4. Influence of control factors on the S/N ratio.

The highest S/N ratio in the response plots represented the optimum SWR. It is apparent that when load as well as abrasion distance rise, the SWR falls. Linear reduction with abrading distance as well as load is similarly visible, although there is a modest difference with the fluctuation as filler loading is reduced. This scenario illustrates the possibility of many wear mechanisms.

Table 5. L_9 orthogonal design and experimental results of the two-body abrasive wear tests.

Filler loading (wt. %)	Load (N)	Abrading distance (m)	Specific wear rate ×10⁻⁹ (m³/Nm)	S/N ratio (dB)
0	5	75	39.47	-31.9253
0	10	150	18.73	-25.4508
0	15	225	10.51	-20.4321
1	5	150	10.76	-20.6362
1	10	225	7.51	-17.5128
1	15	75	9.22	-19.2946
1.5	5	225	9.79	-19.8157
1.5	10	75	20.13	-26.0769
1.5	15	150	9.42	-19.481

The SN ratios are calculated for each of the nine runs. The lowest and highest SN ratios are around -17.51 and -31.92 dB, respectively. They are associated with the first and fifth runs,

respectively. The most optimal mean response was identified to be $A_2B_3C_3$. These findings suggest that G/C/E composites have a slightly lower SWR than controlled C/E composites.

The penetrating capability of SiC abrasive diminishes as abrading distance increases.

Due to their inherent qualities, G/C/E composites exhibit lower SWR than controlled samples. There was a considerable difference amongst them. In a nutshell, the G utilized in this study perform a key role in reducing the SWR, indicating the function of tribo-film was significant. It is well understood that wear resistivity of polymeric composites is determined by the composite's capability to establish a uniform, thin transfer layer on the counter surface. These transfer layers as well as wear fragments accumulate in the abrasive paper fissures or depressions, triggering blockage.

The transfer layer was also noticed for controlled C/E composites, although its adherence to the counter surface was poor, allowing it to be easily dislodged [26]. The optimal set of testing factors for a lower SWR is shown by the main effect plot. This is determined by the main effect plot's slope for every variable. SWR reduces with increasing load as well as abrading distances for all polymeric materials. They are obviously associated with Archard's equation.

Archard's equation is commonly employed to define metal dry sliding wear produced by adhesion, however it has also proven to be quite beneficial in abrasive wear scenarios. The equation is indicated as

$$V = k \frac{L \times D}{H} \qquad (2)$$

wherein V= material's volume loss (m^3), H= hardness, L=load (N), and k=wear coefficient, and D=sliding distance (m). As per the above equation, wear volume is obviously proportionate to both the sliding distance as well as load, while it is conversely proportional to the hardness. Although the apparent contact area is unaffected by the volume loss, the mean size of contact area increases. It has been noted that when the abrading distance rises, harder asperities on the counter face penetrate deeper into the soft specimen surface, while softer asperities flex and shatter more easily [27].

Composites containing 1 wt. % G enhance abrasive wear resist since considerable energy is needed to mitigate failure, as is demonstrated in the current investigation in regard to SWR. However, G/C/E composites outperformed controlled C/E composites in terms of wear resistance [5].

Furthermore, the filler loading as well as adhesion among the G's and polymeric matrix appear to be crucial for wear minimization. For instance, material separation off the specimen surface is made more challenging whenever there's a strong bond among the matrix and fillers, which increases wear resistance. The filler particles' easy separation off the polymer as well as the three-body abrasive caused in contact region, the weak connection amongst the filler particles as well as the polymer matrix is likely to reduce wear resistivity [28]. This is because as the filler fraction rises, there are more filler particles within the transfer film, which disrupts the film owing to the increased hard particles.

Table 6. Response data for S/N ratios under two-body abrasion.

Level	Filler loading (wt. %)	Load (N)	Abrading distance (m)
1	-25.94	-24.13	-25.77
2	-19.15	-23.01	-21.86
3	-21.79	-19.74	-19.25
Delta	6.79	4.39	6.51
Rank	1	3	2

The SN ratio response is shown in Table 6. The delta estimates of the S/N ratio for filler loading, load, and abrading distance are 6.79, 4.39, and 6.59, respectively. Filler loading had the greatest impact on SWR, trailed by abrading distance as well as load.

3.4 Effect of various control factors

Among the control factors, filler loading plays a major role in a material's ability to resist abrasion, with abrading distance coming in second. The SWR is initially high for the abrading distance, load and material class. The SWR drops dramatically when examined against 320 grit size owing to an improvement in the sample's penetrating capabilities [4,29]. As a result of the apparent area of contact being significantly enhanced at higher loads, the SWR decreases with a rise in load from 5 to 10 N. A greater declination trend is also seen when the load is increased from 10 to 15 N. The SWR reduces as the abrading distance is increased [30]. A significant amount of G can interact with the interface as well as distribute the stress as the area of contact is increased [31]. This enables the SWR to reach a constant state or decrease. The SWR is highly dependent on the load, filler loading, as well as abrading distance. Previous research has shown how several parameters affect the filled hybrid polymer composites' abrasive behaviour [32].
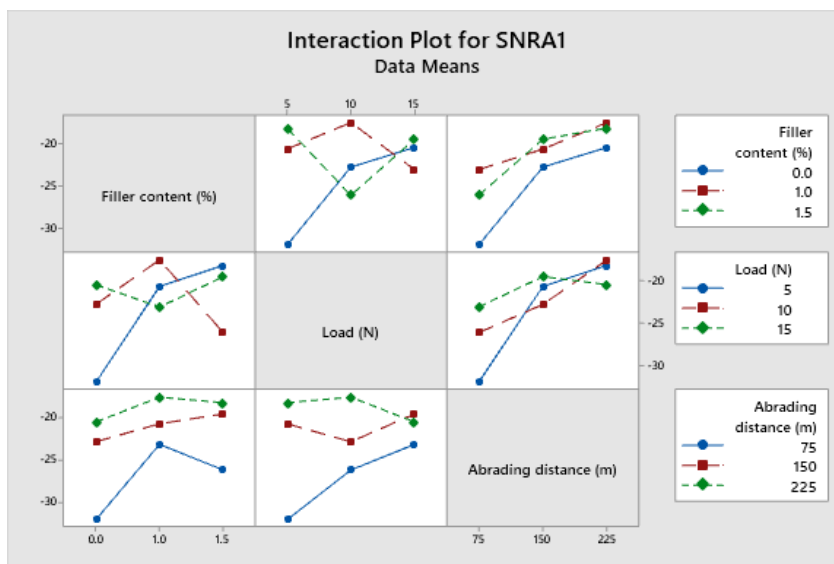
Fig. 5. Interactions plot of SN ratios of GNPs filled carbon epoxy composites.

Any interaction plots with parallel lines indicate the absence of interaction. Lines that are not parallel to one another indicate interaction, and lines that intersect indicate strong interaction. The interaction graph of carbon epoxy composites with G is shown in Fig. 5. The first plot represents the variation of the SN ratio with load, and the second plot is a variation of SN ratios with abrading distance. This gives the interaction of the two control factors (load and abrading distance) by keeping one control factor (filler loading) as a varying parameter. From the first-row graph, it is worth noting that for SN ratio is higher for 1 wt. % of GNPs. Similarly, in the second and third row represents the variation of SN ratios with different control factors. It is seen that there are certain interactions between load and filler loading. Load and abrasion distance are trending upwards. Although a decreased abrading distance leads to the increased SWR, this may be due to the early stages of the wear process.

Fig. 6. Normal probability plot of composites.

Fig. 6 displays the normal probability graph for the samples under investigation together with the cumulative residual distributions. It appears that the error distributions are normal. Despite the fact that the right trials aren't longer relative to the left one, the distribution of errors may be significantly skewed. However, the right side of the trial has few extreme spots owing to the characteristics of the examined samples. The residual often hovers around ±0.5.

3.5 Analysis of variance

Table 7 displays the ANOVA findings for the abrasive wear characteristics of G/C/E composites. This analysis is conducted with a significance level equal to 10% as well as a degree of confidence of ~90%. Table 5 clearly shows that the parameters filler loading, load, as well as abrading distance exhibit statistical and physical relevance on the SWR. As shown in the seventh column of the ANOVA table 7 for G/C/E composites, P of every factor on total variations indicates the level of influence on abrasive wear results. It can be seen that the factors filler loading (P = 36.39%), abrading distance (P = 36.36%), and load (P = 22.97%) have an impact on abrasive wear rates. The error connected with the table of ANOVA results for the means of SN ratio is estimated to be 4.26%. R^2 correlation has been calculated to be 92.10%. The p-value for every individual control parameter is shown in the sixth column of ANOVA table. It is well recognized that the lower the p-value, higher the significance of the associated interaction/factor associated with it.
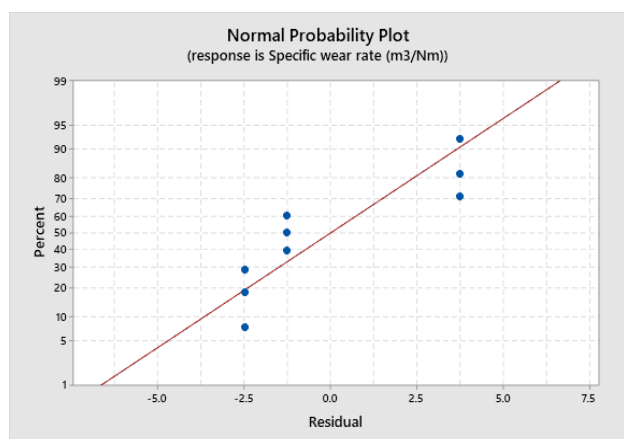
The results from the ANOVA table for the SN ratio (Table 4) shows that filler loading (p = 0.178), abrading distance (p = 0.178), and load (p = 0.29) are the significant controlling variables influencing the SWR of the samples under investigation. It suggests that the filler loading and abrading distance were the most important factors, subsequently followed by applied load. The current work demonstrates the abrasive wear characteristics of epoxy matrix and its composites at abrasive conditions employing the Taguchi technique demonstrates that the abrasive wear characteristic is dependent on the tribological system, filler loading, load, and abrading distance.

3.6 Worn surface morphology

The worn surfaces of controlled C/E composite samples are shown in Fig. 7a and b with a load of 5 N and an abrading distance of 75 m (Table 5, experiment number 1). Fig. 7a shows a scanning electron micrograph of a controlled C/E composite sample abraded with 320 grit SiC paper. The shows plough lines (marked as PL) on the surface, significant matrix degradation (marked as MD in Fig. 7a), carbon fibre exposure (marked as ECF in Fig. 7a) and fibre breaking. These exposed fibres are prone to breakage and removal from the matrix's surface [33]. The ploughing and cutting action of the larger SiC particles severely damage the matrix. Fig. 7a's overall surface topography revealed higher fibre pulverization, fibre breaking, and fibre delamination from the matrix. The photomicrograph also shows matrix fracture propagation and matrix degradation.

Fig. 7b depicts a higher magnification of SEM micrograph of a controlled C/E composite sample that has been abraded using 320 grit abrasive paper. The micrograph also shows deeper ploughing lines (marked as DPL in Fig. 7b) on the surface, greater matrix degradation, and exposure of carbon fibres as well as more fibre breakage (marked as ECFs, and FB in Fig. 7b). The matrix is deteriorating, and additional microcracks may be seen in the micrograph. The photomicrograph also shows a smooth matrix surface with fractures and cavities in some areas. This is because finer abrasive particles are crushed as the abrading distance rises, rendering the SiC particles inoperable. The micrograph also shows loss of the fibre/matrix adhesion (marked as LFMA in Fig. 7b) because of recurrent mechanical stress and fibre debonding from the matrix.

Fig. 8a and b depict the abrasive wear surfaces of 1G/C/E composite samples at 10 N load and 225 m abrading distance (Table 5, experiment number 5). Shallow furrows (marked as SFs in Fig. 8a) are visible in the abrading direction due to ploughing action by sharp abrasive particles. The level of matrix and fibre degradation is smaller in 1G/C/E composite samples than in controlled C/E composite samples (Figs. 7a and b). Significant interactions between fibres and graphene nanoparticles occur in this situation, resulting in improved bonding with the epoxy matrix (marked as GB in Fig. 8a). This conclusion is consistent with the micrograph in Fig. 8a for 1G/C/E composite sample.
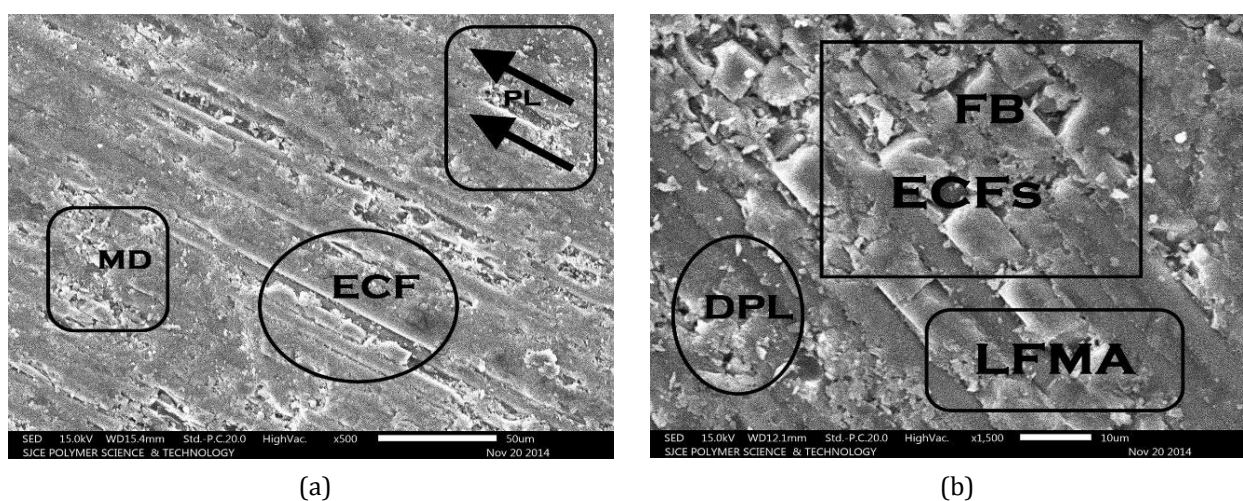

(a)   (b)

Fig. 7. Scanning electron micrographs of the worn surface of controlled C/E composite: (a) 500 X, (b) 1500 X.

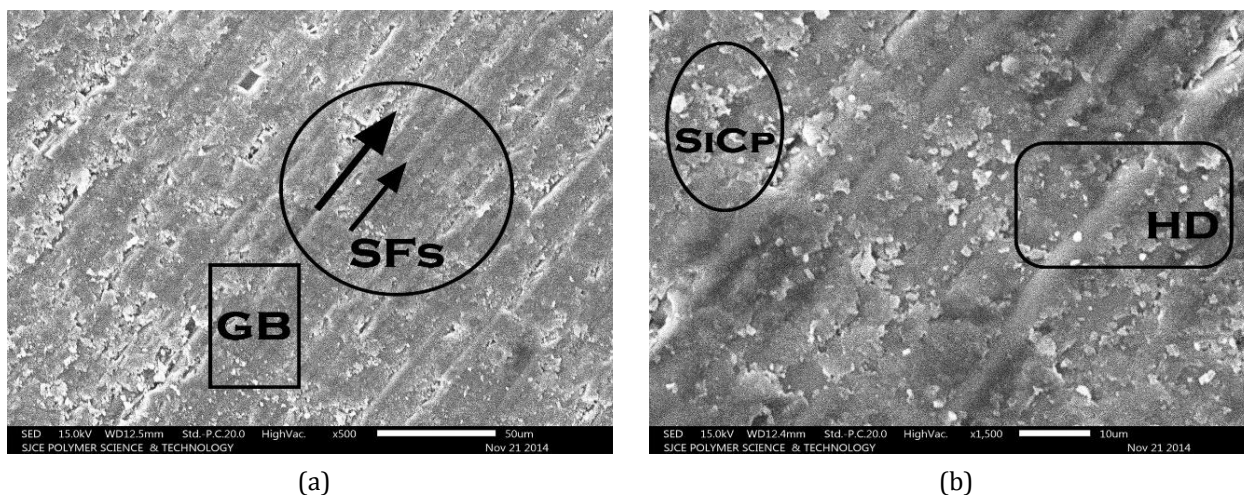(a)   (b)

Fig. 8. Scanning electron micrographs of the worn surface of 1G/ C/E composite: a) 500 X, b) 1500 X.

Table 7. ANOVA table for specific wear rate.

Source	DF	Adj SS	Adj MS	F-Value	P-Value	P (%)
Filler loading (wt. %)	2	300.23	150.12	4.61	0.178	36.39
Load (N)	2	189.53	79.77	2.45	0.29	22.97
Abrading distance (m)	2	299.96	149.98	4.6	0.178	36.36
Error	2	35.18	32.59			4.26
Total	8	824.9				

S = 5.70863 R-Sq = 92.10%

Micrograph at a higher magnification Fig. 8b demonstrates that the graphene nanoparticles and fibres are evidently effectively bound to the epoxy matrix due to their homogeneous dispersion (marked as HD in Fig. 8b). Other worn surface characteristics include the appearance of excellent bonding between the fibre and matrix, as well as a few pulled out SiC particles adhering to the epoxy matrix (marked as SiCp in Fig. 8b). There is also less matrix degradation, less fibre breaking, and very little fibre pull-out from the surface could be seen from Fig. 8b.

The present investigation reveals that the statistical as well as physical significance of the abrasive wear variables and their related interactions (percentage contribution > error) in abrasive wear properties of the fibres are subsequently sheared and later pulled out hybrid nanocomposites. ANOVA results show that fewer interactions are statistically significant but are not physically significant as the corresponding error is greater than the % contribution from the two interactions [34]. This method attributes the fluctuation of variance as well as averages to the absolute values evaluated throughout the experimental runs instead of the parameter's unit value. The influence of variable interaction is

therefore <1%, and its contribution to SWR is relatively less significant [35]. The filler loading is more significant, which might improve the carbon epoxy composite's resistance to abrasion.

3.7 Confirmation Test

The final stage of the DOE approach is a confirmation test. The purpose of a confirmation test run is to validate the findings from the analytical phase [36]. The optimum factor level could be calculated using the prediction equation 2 described below to approximate the estimated S/N ratio for the SWR.

$$\eta_{opt} = U + \sum_{j=1}^{k} (\eta_j - U); \text{ j=1, 2, ...k,} \quad (2)$$

Where, U=Means of all the experimental S/N ratios; j= Means of S/N at optimum factor level; and k=number of significant variables of experimental design that majorly influences the SWR of G/C/E composite.

Table 8. Confirmation test for SWR.

Level	Optimum process parameter $A_2B_3C_3$	
	Predicted value	Experimental value
S/N ratio (dB)	-13.5539	-14.1567
SWR (m^3/Nm)	4.295×10^{-9}	4.9743×10^{-9}

As shown, there is a respectable limit (0.603 dB) disparity between the results of verification as well as calculation. However, the ideal SWR is determined utilizing the significant variables (A_2, B_3, and C_3) from the findings of the ANOVA. The S/N ratio was approximately -13.5539 dB in this instance, and the corresponding SWR value is 4.295×10^{-9} (m^3/Nm). The control parameters A_2, B_3, and C_3, that aren't listed in Table 4 of DOE, were used to predict the SN ratio as well as SWR, and the corresponding SN and SWR values were determined. Table 8 displays the results from the experimental validation employing optimized wear factors, and also a comparison of actual SWR with predicted SWR.

4. CONCLUSIONS

To examine the possible application of GNPs in hybrid nanocomposites, the tribological and mechanical characterization of G/C/E composites were conducted. The findings are summarized as follows:

1. The addition of graphene nanoplatelets (G) enhanced the mechanical properties of C/E composites. Incorporation of 1 wt. % of G increased the hardness and interlaminar shear strength by 14% and 19%, respectively, as compared to C/E composites,

2. The Taguchi experimental design approach allows us to efficiently study the two-body abrasive wear behaviour of C/E and its nanocomposites. The percentage contributions to the two-body abrasive wear performances of the G/C/E hybrid composites are listed in the following order: Load (P = 22.97%) >>> Filler loading (P = 36.39%) >>> Abrading distance (P = 36.36%) >>> Load (P = 36.39%).

3. The combination of control factors A2, B3, and C3 results in a reduced SWR. The experimentally measured value of the S/N ratio was observed to closely match with the predicted of the carbon epoxy nanocomposite samples with <5% error.

4. Graphene nanoplatelets might be considered as a viable reinforcing material with high wear resistance for a variety of tribological applications.

REFERENCES

[1] K. P. Matabola, A. R. De Vries, F. Moolman, and A. S. Luyt, "Single polymer composites: a review," *Journal of Materials Science*, vol. 44, no. 23, pp. 6213–6222, Dec. 2009, doi: 10.1007/s10853-009-3792-1.

[2] M. M. Zagho, E. A. Hussein, and A. A. Elzatahry, "Recent overviews in functional polymer composites for biomedical applications," *Polymers*, vol. 10, no. 7, p. 739, Jul. 2018, doi: 10.3390/polym10070739.

[3] S. M. Darshan and B. Suresha, "Effect of basalt fiber hybridization on mechanical properties of silk fiber reinforced epoxy composites," *Materials Today: Proceedings*, vol. 43, pp. 986–994, Jan. 2021, doi: 10.1016/j.matpr.2020.07.618.

[4] B. Suresha, G. Chandramohan, Siddaramaiah, P. Samapthkumaran, and S. Seetharamu, "Three-body abrasive wear behaviour of carbon and glass fiber reinforced epoxy composites," *Materials Science and Engineering: A*, vol. 443, no. 1–2, pp. 285–291, Jan. 2007, doi: 10.1016/j.msea.2006.09.016.

[5] B. Suresha and K. N. S. Kumar, "Investigations on mechanical and two-body abrasive wear behaviour of glass/carbon fabric reinforced vinyl ester composites," *Materials in Engineering*, vol. 30, no. 6, pp. 2056–2060, Jun. 2009, doi: 10.1016/j.matdes.2008.08.038.

[6] N. Shahid, R. G. Villate, and A. R. Barron, "Chemically functionalized alumina nanoparticle effect on carbon fiber/epoxy composites," *Composites Science and Technology*, vol. 65, no. 14, pp. 2250–2258, Nov. 2005, doi: 10.1016/j.compscitech.2005.04.001.

[7] K. Kumaresan, G. Chandramohan, M. Senthilkumar, B. Suresha, and S. Indran, "Dry Sliding Wear Behaviour of Carbon Fabric-Reinforced Epoxy Composite with and without Silicon Carbide," *Composite Interfaces*, vol. 18, no. 6, pp. 509–526, Jan. 2011, doi: 10.1163/156855411x610241.

[8] S. M. Darshan, B. Suresha, and I. M. Jamadar, "Optimization of Abrasive Wear Parameters of Halloysite Nanotubes Reinforced Silk/Basalt Hybrid Epoxy Composites using Taguchi Approach," *Tribology in Industry*, vol. 44, no. 1, pp. 253–267, Jun. 2022, doi: 10.24874/ti.1131.06.21.08.

[9] S. M. Darshan and B. Suresha, "Effect of halloysite nanotubes on Physico-Mechanical Properties of Silk/Basalt fabric reinforced epoxy composites," *Materials Science Forum*, vol. 1048, pp. 21–32, Jan. 2022, doi: 10.4028/www.scientific.net/msf.1048.21.

[10] V. Pejakovi, R. Jisa, and F. Franek, "Abrasion Resistance of Selected Commercially Available Polymer Materials," *Tribologia-Finnish Journal of Tribology*, vol. 1, no. 1, pp. 21–27, Jul. 2015.

[11] P. H. Shipway and N. K. Ngao, "Microscale abrasive wear of polymeric materials," *Wear*, vol. 255, no. 1–6, pp. 742–750, Aug. 2003, doi: 10.1016/s0043-1648(03)00106-6.

[12] V. K. Thakur, *Green Composites from Natural Resources*. Engineering & Technology, Physical Sciences, Boca Raton, 2013. doi: 10.1201/b16076.

[13] M. C. Scedil *et al.*, "A brief overview on synthesis and applications of graphene and graphene-based nanomaterials," *Frontiers of Materials Science*, vol. 13, no. 1, pp. 23–32, Jan. 2019, doi: 10.1007/s11706-019-0452-5.

[14] F. Wang, L. T. Drzal, Y. Qin, and H. Zhang, "Size effect of graphene nanoplatelets on the morphology and mechanical behavior of glass fiber/epoxy composites," *Journal of Materials Science*, vol. 51, no. 7, pp. 3337–3348, Dec. 2015, doi: 10.1007/s10853-015-9649-x.

[15] S. Kumar, K. K. Singh, and J. Ramkumar, "Comparative study of the influence of graphene nanoplatelets filler on the mechanical and tribological behavior of glass fabric-reinforced epoxy composites," *Polymer Composites*, vol. 41, no. 12, pp. 5403–5417, Sep. 2020, doi: 10.1002/pc.25804.

[16] S. Kumar, K. K. Singh, and J. Ramkumar, "The effects of graphene nanoplatelets on the tribological performance of glass fiber-reinforced epoxy composites," *Proceedings of the Institution of Mechanical Engineers, Part J: Journal of Engineering Tribology*, vol. 235, no. 8, pp. 1514–1525, Oct. 2020, doi: 10.1177/1350650120965756.

[17] A. K. Srivastava, V. Gupta, C. S. Yerramalli, and A. Singh, "Flexural strength enhancement in carbon-fiber epoxy composites through graphene nano-platelets coating on fibers," *Composites Part B: Engineering*, vol. 179, p. 107539, Dec. 2019, doi: 10.1016/j.compositesb.2019.107539.

[18] H. R. Shivakumar, N. M. Renukappa, K. Shivakumar, and B. Suresha, "The reinforcing effect of graphene on the mechanical properties of Carbon-Epoxy composites," *Open Journal of Composite Materials*, vol. 10, no. 02, pp. 27–44, Jan. 2020, doi: 10.4236/ojcm.2020.102003.

[19] A. Namdev, A. Telang, and R. Purohit, "Effect of graphene nano platelets on mechanical and physical properties of Carbon Fibre/Epoxy hybrid composites," *Advances in Materials and Processing Technologies*, vol. 8, no. sup3, pp. 1168–1181, Jun. 2021, doi: 10.1080/2374068x.2021.1939557.

[20] A. Namdev, A. Telang, and R. Purohit, "Experimental investigation on mechanical and wear properties of GNP/Carbon fiber/epoxy hybrid composites," *Materials Research Express*, vol. 9, no. 2, p. 025303, Feb. 2022, doi: 10.1088/2053-1591/ac4e3f.

[21] Vinod, A. Kumar, B. Suresha, M. Kumar, and S. Ramesh, "Study on Two Body Abrasive Wear behaviour of Carboxyl-Graphene Reinforced Epoxy Nano-composites," *IOP Conference Series: Materials Science and Engineering*, vol. 376, p. 012058, Jun. 2018, doi: 10.1088/1757-899x/376/1/012058.

[22] A. Namdev, R. Purohit, and A. Telang, "Impact of graphene nano particles on tribological behaviour of carbon fibre reinforced composites," *Advances in Materials and Processing Technologies*, pp. 1–18, Mar. 2023, doi: 10.1080/2374068x.2023.2189670.

[23] A. Namdev, A. Telang, R. Purohit, and M.K. Agrawal, "An experimental assessment of abrasive wear behavior of GNP/Carbon fiber/epoxy hybrid composites," Indian Journal of Engineering and Materials Sciences, vol. 29, no. 6, pp. 777–785, 2022, doi: 10.56042/ijems.v29i6.70309.

[24] P. Akangah and K. Shivakumar, "Impact damage resistance and tolerance of polymer nanofiber interleaved composite laminates," *53rd AIAA/ASME/ASCE/AHS/ASC Struct. Struct. Dyn. Mater. Conf.* Apr. 2012, doi: 10.2514/6.2012-1374.

[25] F. Yan *et al.*, "A novel π bridging method to graft graphene oxide onto carbon fiber for interfacial enhancement of epoxy composites," *Composites Science and Technology*, vol. 201, p. 108489, Jan. 2021, doi: 10.1016/j.compscitech.2020.108489.

[26] A. Chira, A. Kumar, T. Vlach, L. Laiblová, A. S. Škapin, and P. Hájek, "Property improvements of alkali resistant glass fibres/epoxy composite with nanosilica for textile reinforced concrete applications," *Materials & Design*, vol. 89, pp. 146–155, Jan. 2016, doi: 10.1016/j.matdes.2015.09.122.

[27] A. P. Harsha and U. S. Tewari, "Tribo performance of polyaryletherketone composites," *Polymer Testing*, vol. 21, no. 6, pp. 697–709, Jan. 2002, doi: 10.1016/s0142-9418(01)00145-3.

[28] C. J. Schwartz and S. Bahadur, "The role of filler deformability, filler–polymer bonding, and counterface material on the tribological behavior of polyphenylene sulfide (PPS)," *Wear*, vol. 251, no. 1–12, pp. 1532–1540, Oct. 2001, doi: 10.1016/s0043-1648(01)00799-2.

[29] H. Unal, U. Şen, and A. Mimaroğlu, "Abrasive wear behaviour of polymeric materials," *Materials in Engineering*, vol. 26, no. 8, pp. 705–710, Jan. 2005, doi: 10.1016/j.matdes.2004.09.004.

[30] Y. Şahin, "Analysis of abrasive wear behavior of PTFE composite using Taguchi's technique," *Cogent Engineering*, vol. 2, no. 1, p. 1000510, Jan. 2015, doi: 10.1080/23311916.2014.1000510.

[31] C. Anand and S. Kumaresh, "Influence of titanium carbide on the three- body abrasive wear behaviour of Glass-Fabric reinforced epoxy composites," *Advances in Materials*, vol. 1, no. 1, p. 9, Jan. 2012, doi: 10.11648/j.am.20120101.12.

[32] C. Liu, L. Ren, R. D. Arnell, and T. Jin, "Abrasive wear behavior of particle reinforced ultrahigh molecular weight polyethylene composites," *Wear*, vol. 225–229, pp. 199–204, Apr. 1999, doi: 10.1016/s0043-1648(99)00011-3.

[33] B. K. Muralidhara, S. P. K. Babu, G. Hemanth, and B. Suresha, "Optimization of abrasive wear behaviour of halloysite nanotubes filled carbon fabric reinforced epoxy hybrid composites," *Surface Topography: Metrology and Properties*, vol. 8, no. 4, p. 045028, Dec. 2020, doi: 10.1088/2051-672x/abc8e1.

[34] S. M. Darshan and B. Suresha, "Mechanical and abrasive wear behaviour of waste silk fiber reinforced epoxy biocomposites using Taguchi method," *Materials Science Forum*, vol. 969, pp. 787–793, Aug. 2019, doi: 10.4028/www.scientific.net/msf.969.787.

[35] S. R. Chauhan, A. Kumar, I. Singh, and P. S. Kumar, "Effect of fly ash content on friction and dry sliding wear behavior of glass fiber reinforced polymer composites - a Taguchi approach," *Journal of Minerals and Materials Characterization and Engineering*, vol. 09, no. 04, pp. 365–387, Jan. 2010, doi: 10.4236/jmmce.2010.94027.

[36] E. R. Ziegel and P. Ross, "Taguchi Techniques for Quality Engineering," *Technometrics*, vol. 39, no. 1, p. 109, Feb. 1997, doi: 10.2307/1270793.